:UMENTATION PAGE

Form Approved
OMB No. 0704-0188

AD-A233 612

2. REPORT DATE	3. REPORT TYPE AND DATES COVERED
2/11/91	

4. TITLE AND SUBTITLE
Interaction of Ba Atoms and Ba^+ Ions with Inert Gases

5. FUNDING NUMBERS
DAAL03-87-K-0068

6. AUTHOR(S)
Keith D. Bonin and Will Happer

7. PERFORMING ORGANIZATION NAME(S) AND ADDRESS(ES)
Dept. of Physics
Princeton University
Princeton, NJ 08544

8. PERFORMING ORGANIZATION REPORT NUMBER

9. SPONSORING/MONITORING AGENCY NAME(S) AND ADDRESS(ES)
U. S. Army Research Office
P. O. Box 12211
Research Triangle Park, NC 27709-2211

10. SPONSORING/MONITORING AGENCY REPORT NUMBER
ARO 24511.6-PH

11. SUPPLEMENTARY NOTES
The view, opinions and/or findings contained in this report are those of the author(s) and should not be construed as an official Department of the Army position, policy, or decision, unless so designated by other documentation.

12a. DISTRIBUTION/AVAILABILITY STATEMENT
Approved for public release; distribution unlimited.

12b. DISTRIBUTION CODE

13. ABSTRACT *(Maximum 200 words)*

This report describes four different experiments. The majority of the experiments involve the interaction of Ba and Ba^+ with each other, with noble gas atoms, with electrons, and with electromagnetic fields.

14. SUBJECT TERMS
Metastable deexcitation, absolute photoionization cross section, focused particle beams, changing fluorescence of a Beam in a magnetic field.

15. NUMBER OF PAGES
15

16. PRICE CODE

17. SECURITY CLASSIFICATION OF REPORT	18. SECURITY CLASSIFICATION OF THIS PAGE	19. SECURITY CLASSIFICATION OF ABSTRACT	20. LIMITATION OF ABSTRACT
UNCLASSIFIED	UNCLASSIFIED	UNCLASSIFIED	UL

NSN 7540-01-280-5500
Standard Form 298 (Rev 2-89)
Prescribed by ANSI Std 239-18
298-102

ARO 24511.6-PH

Interaction of Ba Atoms and Ba^+ Ions with Inert Gases

Final Report

Keith D. Bonin and Will Happer

Keith D. Bonin W. Happer

U.S. Army Research Office

Grant DAAL03-87-K-0068

Department of Physics
Princeton University
Princeton, New Jersey 08544

Table of Contents

1. List of Figures

Fig. 1. Timing sequence for measuring photoionization cross sections by fluorescence reduction. The exciting and photoionizing laser pulses are shown at the top. The middle curve shows the fluorescent intensity $I_f(t)$ produced as atoms decay from the initial excited level to a lower-lying level. The photoionization pulse decreases this fluorescence due to removal of atoms from the excited fluorescing state. The bottom plot shows the integration times for integrating the fluorescence before (interval $T_1 \lesssim \tau/3$) and after (interval $T_2 \simeq 3\tau$) the photoionizing pulse is applied. The signal S_1 is used as a normalization for the signal S_2. The integrations are performed using 2 independent gated integrators.

Fig. 2. A plot of the Cs $7D_{3/2}$ photoionization cross section measured at 6 different photon energies. The solid curve is a quantum defect theory calculation of the photoionization cross section.

Fig. 3. Two-stage laser ablation. (a) In the first stage the ablating laser is pulsed when the barium has rotated into place under a transparent substrate. The vertical distance between the solid barium slab and the substrate is 0.2-0.5 cm. Material is removed from the slab of barium and is deposited onto the substrate. (b) The laser is pulsed again when a hole in the rotating stage is in position, ablating the barium deposited on the substrate and forming a beam which propagates through the hole. Material deposited on a cylindrically or spherically curved glass substrate is focused to the center of curvature of the substrate. A quartz crystal microbalance (QCM) is used to measure the total mass deposited by the focused barium beam.

Fig. 4. Spatial distribution of mass in the second-stage ablation beam. (a) Three-dimensional surface plot of the thickness of barium at the focus of the second-stage ablation beam. The data presented is for 152 ± 2 pulses of the barium beam, at a distance of 10.7 cm. The thickness is measured in terms of the attenuation length d defined in Eq. (3). (b) Radial plot of the data of (a). This plot was made by assuming that the data shown in (a) was axially symmetric about the center of mass of the distribution. The data was averaged for 200 equally spaced radial intervals.

Fig. 5. Fluorescent intensities versus wavelength over the spectral region from 4000 Å to 5200 Å with (a) B=0 G, and (b) B=190 G. The low-lying Ba^+ lines clearly dominate the spectrum at high field values, whereas the many high-lying ion and neutral lines that were present at B=0 G are entirely absent at B=190 G. The scale in (a) is five times more sensitive than that for (b). Lines are labelled according to the measurements made from strip chart recordings - the actual wavelengths of the lines may differ slightly from these.

Fig. 6. A plot of the fluorescent intensity of the Ba $6s6p\ ^1P_1 \rightarrow 6s^2\ ^1S_0$ line at 5537 Å as a function of magnetic field. This line showed a large decrease in intensity to a minimum and a subsequent increase in fluorescence with increasing magnetic field; other lines showed quite different behavior.

2. Main Report

This report consists of four brief sections describing the work completed with the financial support provided by this grant. The majority of experiments involve the interaction of Ba and Ba^+ with each other, with noble gas atoms, with electrons, and with electromagnetic fields.

2.1 Relaxation of Ba^+ Metastables

Problem studied: We investigated the deactivation mechanisms of the metastable Ba^+ 5 $^2D_{3/2}$ level for the case where a barium plasma was created in a helium-gas background. The motivation for this work was twofold. First, to help clarify the very important, but poorly understood, phenomena that limit the average power output and pulse duration of discharge lasers - lasers having metastable atoms as the final state of the lasing transition. Secondly, they play a significant role in proposed schemes for efficiently spin-polarizing ^3He nuclei via spin-exchange with spin-polarized Ba^+ in a Ba^+He molecule.

Results: To study Ba^+ in He as unambiguously as possible, we produced the Ba^+ by photoionization with a pulsed dye laser. This allowed for variation of the electron density independent of the He density of the Ba density. We measured the deexcitation rates of the $Ba^+(5\ ^2D_{3/2})$ state in He buffer gas at densities of about 1 amagat and in the temperature range of 500-650 °C. We found that an important deexcitation mechanism is superelastic scattering with the electrons in the plasma, i.e.

$$e^- + Ba^+(5^2D_{3/2}) \rightarrow e^- + Ba^+(6^2S_{1/2}) + \Delta E, \qquad (1)$$

where ΔE= 4674 cm^{-1} is the excitation energy of the $Ba^+(5\ ^2D_{3/2})$ state. Using the principle of detailed balance, we deduced an electron-impact excitation cross section of 11±4.9 $Å^2$. After subtracting off the contribution of superelastic collisions with neutral Ba atoms, i.e.,

$$Ba + Ba^+(5^2D_{3/2}) \rightarrow Ba + Ba^+(6^2S_{1/2}) + \Delta E, \qquad (2)$$

we obtained a cross section of $\sigma_{Ba} = 130 \pm 25$ $Å^2$. This large cross section is reasonable due to the low energy of 5 $^2D_{3/2}$ state and the repulsive nature of the lowest $^2\Sigma_g^+$ potential curve of Ba_2^+. Finally, we observed no dependence of the deexcitation rate on the He density, and we inferred an upper limit on the deexcitation cross section of $\sigma_{He} \leq 130 \pm 9 \times 10^{-22}$ cm^2. This cross section is more than four orders of magnitude smaller than that reported by some earlier researchers. We believe their numbers are in error, perhaps due to impurities in their apparatus.

2.2. Absolute Photoionization Cross Sections of the Cs 7 $D_{3/2}$ Level Measured Using Fluorescence Reduction

Problem studied: To find a simple technique for measuring the absolute photoionization cross sections of excited atoms. The motivation for this work was to experimentally test theoretical predictions that Cooper minima in the photoionization cross sections of excited

states are more numerous than for ground states. In some cases, such minima were predicted to occur in the visible region of the optical spectrum.

Results: We developed a new technique for measuring absolute photoionization cross sections of excited atoms[1]. This method relies on a measurement of the reduced fluorescence of the excited atomic level resulting from photoionization. Cross sections were measured for the Cs $7D_{3/2}$ level at 6 different photon energies.

Our method works in the following way. Excited atoms are created by some process - in our case by two photon absorption of light from a pulsed dye laser. The excited atoms radiatively decay with a mean lifetime τ. The intensity in one of the fluorescing lines is temporally integrated until a second laser pulse photoionizes some of the excited atoms. The second laser, with pulsewidth $\Delta t_2 \ll \tau$ reduces the number of fluorescing atoms by photoionization. The subsequent fluorescence, after passage of the photoionizing laser pulse, is then integrated for a few lifetimes. The sequence of events is given in Fig.1.

We ratio the two integrated fluorescent signals $R=S_2/S_1$ to reduce shot-to-shot intensity fluctuations due to variations in excitation laser power. This ratio is proportional to $\exp(-F\sigma/h\nu)$ in the case of a uniform photoionizing laser beam or to $(1 + F\sigma/h\nu)^{-1}$ in the case of a speckled beam, where F is the fluence (energy/area) of the photoionizing laser pulse, $h\nu$ is the photon energy, and σ is the photoionization cross section. By varying the fluence F, a photoionization curve can be generated that can be fit to one of the functions above with only one free parameter: σ. The ionizing laser is linearly polarized at the magic angle ($\theta = 54.7°$) with respect to the quantization axis to ensure the ionization probability is independent of magnetic sublevel population. The fluorescence is collected at right angles to the quantization axis with polarization at the magic angle with respect to the quantization axis. This insures that the observed fluorescence is proportional to the total number of excited atoms in all magnetic sublevels of the excited state. For these polarizations, significant changes in the magnetic sublevel populations that occur under many experimental conditions are unimportant and will not affect the final result.

The measured Cs $7D_{3/2}$ photoionization cross sections are plotted in Fig. 2. The solid curve represents cross sections we calculated using expressions derived from a quantum defect theory analysis made by Burgess and Seaton[2]. In terms of a very important figure of merit, the ratio of the energy range of the free electron to its original binding energy in the atom, our data is the best set of measurements ever reported.

We emphasize the technique's simplicity. It uses a simple, closed cell, not a cumbersome vacuum system. It utilizes a straightforward fluorescence measurement made using a photomultiplier tube and two gated integrators. The data is fit to an elementary function that depends on the choice of laser fluence distribution. The result is an efficient and accurate measurement of the absolute photoionization cross section of an excited atomic state.

2.3. Focused Particle Beams Produced by Two-stage Laser Ablation

Problem studied: To establish a technique for producing well-collimated, high density beams of refractory-metal atoms. Improvement in the density of atomic beams as well

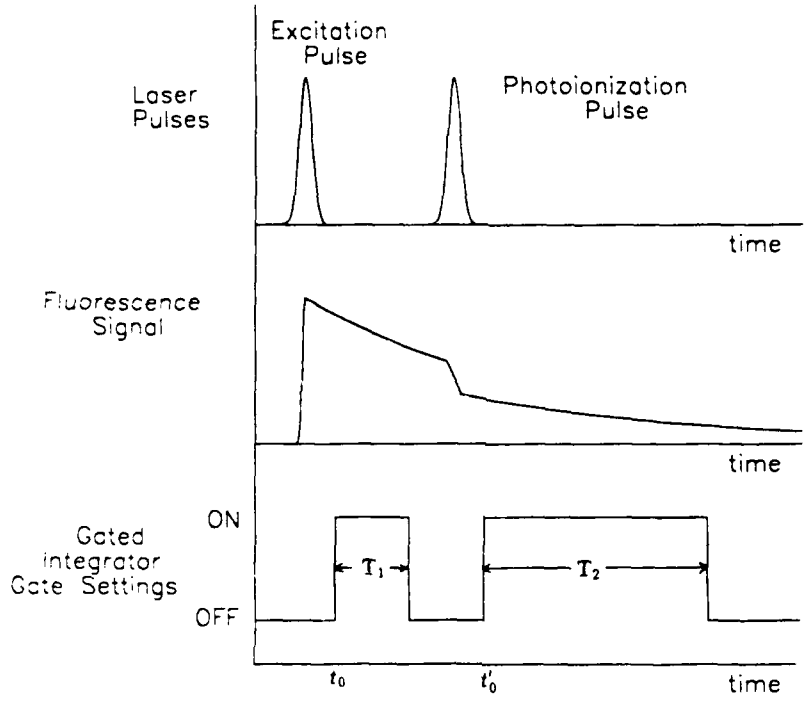

$$S_1 = \int_{t_0}^{t_0-T_1} I_f(t)dt \qquad S_2 = \int_{t_0'}^{t_0'+T_2} I_f(t)dt$$

Figure 1: Timing sequence for measuring photoionization cross sections by fluorescence reduction. The exciting and photoionizing laser pulses are shown at the top. The middle curve shows the fluorescent intensity $I_f(t)$ produced as atoms decay from the initial excited level to a lower-lying level. The photoionization pulse decreases this fluorescence due to removal of atoms from the excited fluorescing state. The bottom plot shows the integration times for integrating the fluorescence before (interval $T_1 \lesssim \tau/3$) and after (interval $T_2 \simeq 3\tau$) the photoionizing pulse is applied. The signal S_1 is used as a normalization for the signal S_2. The integrations are performed using 2 independent gated integrators.

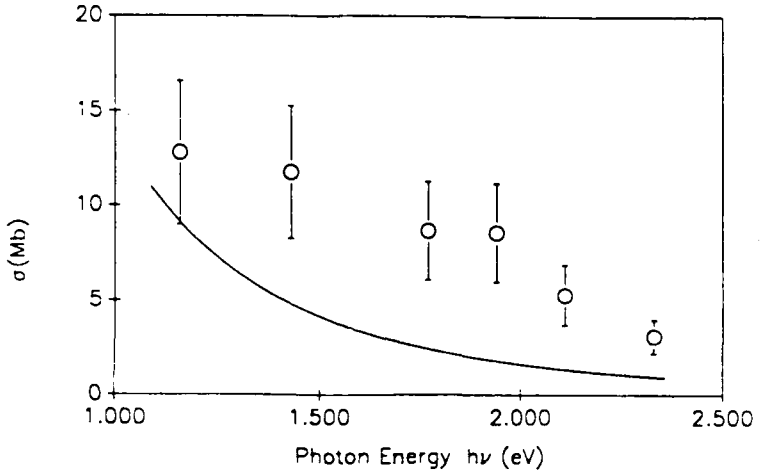

Figure 2: A plot of the Cs $7D_{3/2}$ photoionization cross section measured at 6 different photon energies. The solid curve is a quantum defect theory calculation of the photoionization cross section.

as a reduction in their mean transverse temperature would be generally useful for many fundamental experiments in atomic physics and chemistry. Our immediate interest was to produce a cold, dense beam of barium which was needed to begin work on a new technique for measuring atomic polarizabilities of refractory-metal atoms.

Results: We developed a system for focusing laser ablated particle beams. The focused beam consisted of neutrals, ions, and clusters.[3] Using this technique we have produced a collimated beam and beams which were focused in one and two dimensions. The on-axis density was 5×10^{15} particles/cm^3 for a barium beam focused in two dimensions over a distance of 10.7 cm and 10^{15} particles/cm^3 for a collimated beam at the same distance. It may be possible to choose the energy and duration of the ablating laser to produce beams which are predominantly composed of clusters, ions, or neutrals.

The method by which focused beams are produced is illustrated in Fig. 3. The mass flux distribution of the beam is determined by depositing barium onto a glass plate. The plate is rotated 90° and illuminated by a source of monochromatic light. The transmitted light is imaged onto a commercial CCD camera. The image is digitized and stored by a frame grabber and transferred to nonvolatile memory on a personal computer for analysis. A qualitative measure of the average thickness of barium at a given location on the image is determined by assuming that the transmitted intensity is of the form

$$T(h)/T(0) = \exp -h/d \tag{3}$$

where h is the thickness and d is a characteristic attenuation length. The spatial distribution of mass for a focused beam of barium is shown in Fig. 4. From this data we may estimate a radius at half-maximum of 0.18 cm at a distance of 10.7 cm. This indicates that the ratio of

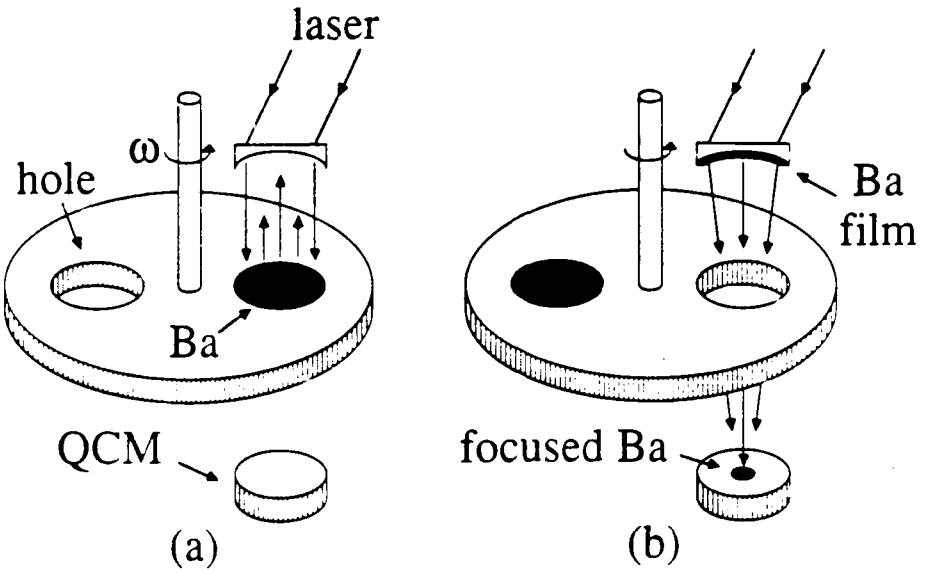

Figure 3: Two-stage laser ablation. (a) In the first stage the ablating laser is pulsed when the barium has rotated into place under a transparent substrate. The vertical distance between the solid barium slab and the substrate is 0.2-0.5 cm. Material is removed from the slab of barium and is deposited onto the substrate. (b) The laser is pulsed again when a hole in the rotating stage is in position, ablating the barium deposited on the substrate and forming a beam which propagates through the hole. Material deposited on a cylindrically or spherically curved glass substrate is focused to the center of curvature of the substrate. A quartz crystal microbalance (QCM) is used to measure the total mass deposited by the focused barium beam.

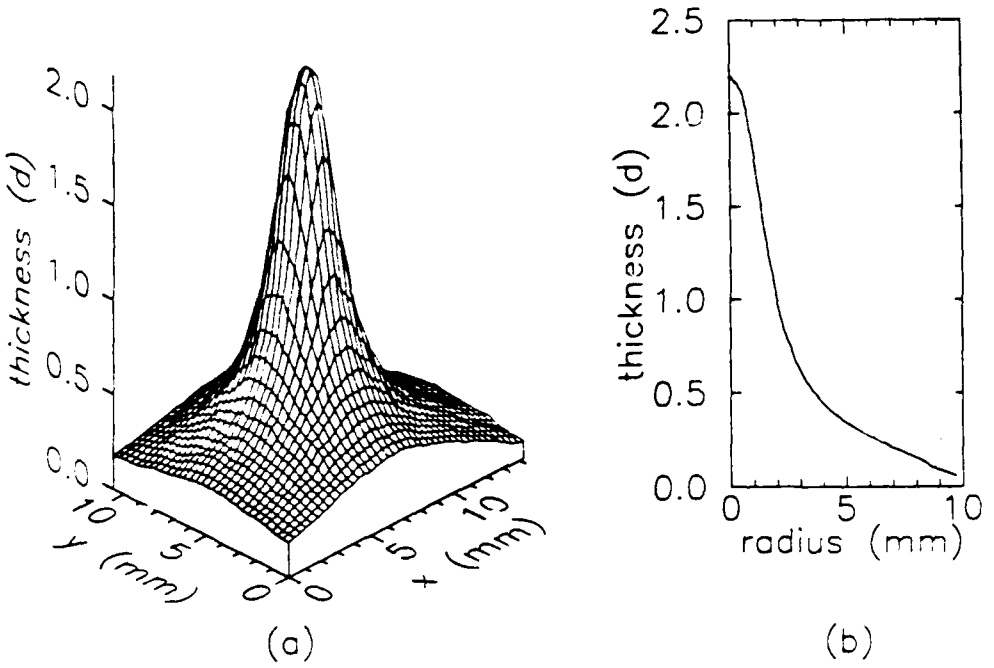

Figure 4: Spatial distribution of mass in the second-stage ablation beam. (a) Three-dimensional surface plot of the thickness of barium at the focus of the second-stage ablation beam. The data presented is for 152 ± 2 pulses of the barium beam, at a distance of 10.7 cm. The thickness is measured in terms of the attenuation length d defined in Eq.3. (b) Radial plot of the data of (a). This plot was made by assuming that the data shown in (a) was axially symmetric about the center of mass of the distribution. The data was averaged for 200 equally spaced radial intervals.

transverse to longitudinal velocities will be on the order of 2×10^{-2} for a collimated beam.

The number density, n, of a particle beam is estimated as $n = N/(Av\Delta t)$, where N is the total number of particles in a single pulse of velocity v, area A, and spread in time of Δt. A quartz crystal microbalance was used to directly measure N. The time dependence of the fluorescence at known distances for ablation from a solid target was used to estimate a longitudinal velocity and corresponding spread of $(3\pm1)\times10^5$ cm/s. We make the assumption that this is also the velocity of a particle beam formed by ablation from a thin film. Using values quoted above we may estimate a number density of 5×10^{15} particles/cm^3 at the focus of the focused beam.

Two-stage laser ablation is a promising method for producing particle beams. The number densities achieved with our technique are many orders of magnitude greater than those attainable with an effusive oven source. In addition the vacuum load is much smaller for two-stage laser ablation since it is a pulsed process. Although our studies have been carried out with barium this method of producing focused particle beams is expected to be independent of element and somewhat independent of the wavelength of the ablating laser. The focusing characteristics of the beam are easily controlled and may be changed to suit each particular application.

2.4. Changing Fluorescence in a Laser-produced Barium Beam due to an Axial Magnetic Field

Problem studied: To elucidate the fundamental mechanisms which produce changes in fluorescence of an atomic and ionic beam, formed by laser ablation, in a magnetic field. These mechanisms might explain the previously reported attenuation and enhancements in low-density plasmas, such as those found in lamps[4]. The physical mechanisms responsible for these observations, as well as those responsible for the improved efficacy of discharge lamps placed in a magnetic field, are poorly understood.

Results: We performed quantitative measurements of the changing fluorescence of a laser-produced barium beam in an axial magnetic field[5]. The dramatic changes in fluorescence that occur when a small magnetic field is applied can be seen in Fig. 5. Under modest magnetic fields the principal lines of Ba^+ at 4935 Å and 4555 Å dominate the spectrum in this region. The peak intensity of the 4935 Å line was 14 times larger for B=190 G than for B=0 G fields and 70 times larger for B=300 G than for B=0 G fields.

Time-integrated intensities have been measured as a function of increasing magnetic field for 14 lines of neutral and singly ionized barium. The lines can be categorized according to the shape of their intensity versus magnetic field curves. Three qualitatively different intensity-field curves were observed: extinction - the higher-lying ion and neutral transitions exhibited a sharp decrease in intensity with increasing field; growth - the low-lying ion lines show a large increase in intensity with increasing field; minima - the low-lying neutral lines first decrease in intensity, reach a minimum, and then grow in intensity for larger fields. An example of the last type is given in Fig. 6.

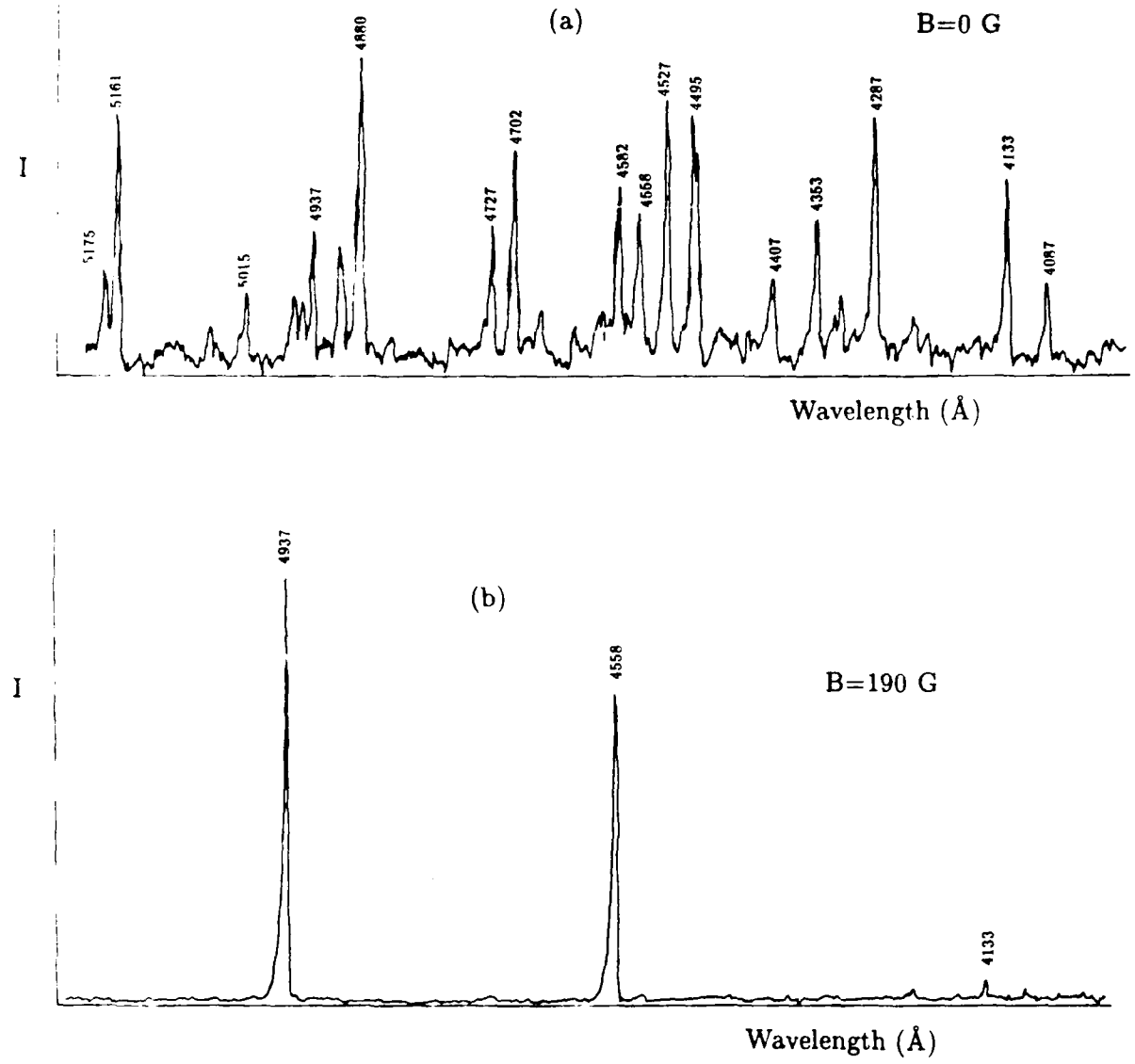

Figure 5: Fluorescent intensities versus wavelength over the spectral region from 4000 Å to 5200 Å with (a) B=0 G, and (b) B=190 G. The low-lying Ba^+ lines clearly dominate the spectrum at high field values, whereas the many high-lying ion and neutral lines that were present at B=0 G are entirely absent at B=190 G. The scale in (a) is five times more sensitive than that for (b). Lines are labelled according to the measurements made from strip chart recordings – the actual wavelengths of the lines may differ slightly from these.

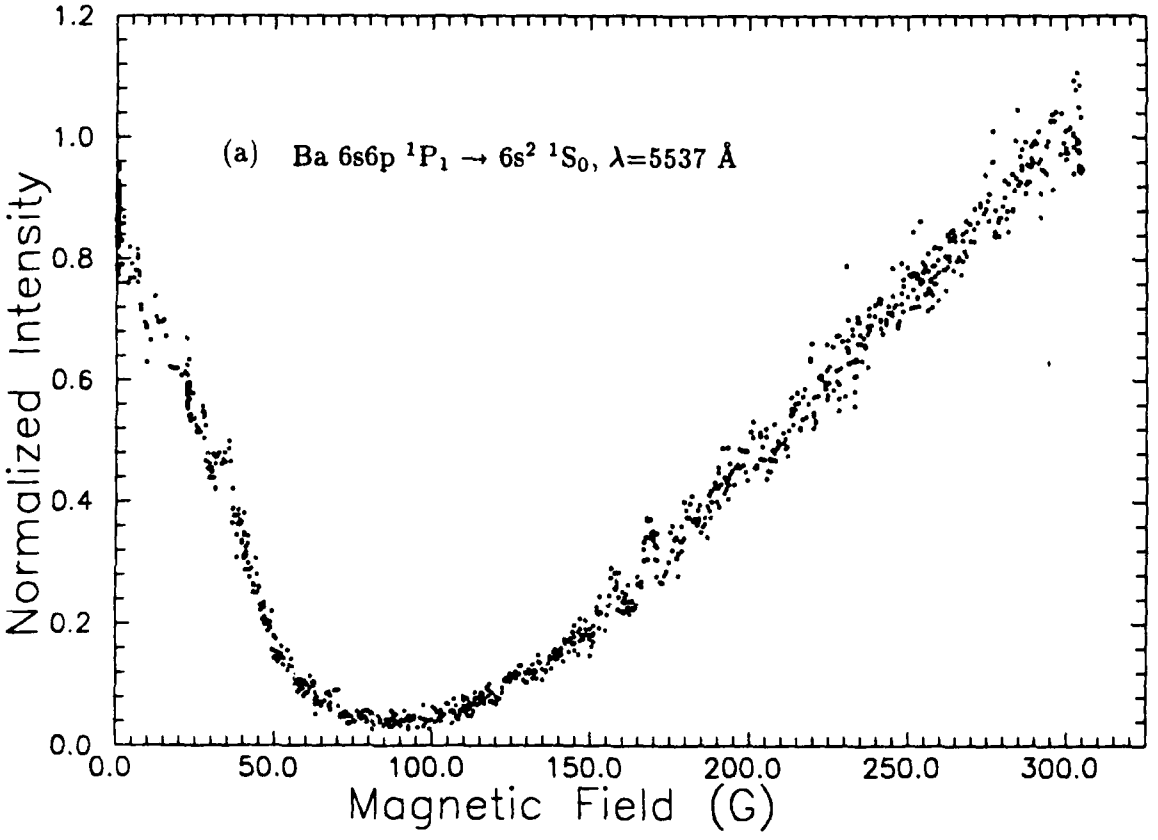

Figure 6: A plot of the fluorescent intensity of the Ba $6s6p\ ^1P_1 \rightarrow 6s^2\ ^1S_0$ line at 5537 Å as a function of magnetic field. This line showed a large decrease in intensity to a minimum and a subsequent increase in fluorescence with increasing magnetic field; other lines showed quite different behavior.

In addition, simple diagnostics were used to measure the important characteristics of the beam 10 cm downstream from the source: electron density and temperature; neutral atom density and timing; ion density and timing. A charge-coupled camera, a Langmuir probe, a tunable diode laser, and a line fluorescence detection system were used to investigate the beam-field interaction.

The changes in fluorescence spectra are speculated to be due to field-varying electron-neutral and electron-ion collisions. For low electron and ion densities the magnetic field permeates the bulk of the plasma even at the highest field strengths. In an axial magnetic field the electrons will have the same longitudinal speed as before, but, instead of colliding with the walls, they will execute gyro orbits and collide with neutral atoms and ions. The increase in collisions due to such confinement is the primary physical effect that *significantly* alters the fluorescence with increasing magnetic field. The measurements support a model in which the energy lost by the quenched higher-lying levels excites lower-lying levels using electrons as an intermediary. Further investigation is needed to verify the model's assumptions and to provide a calculated fit of the intensity-field curves.

2.5. List of All Publications

1. K. D. Bonin, D. P. Saltzberg, W. Happer, Phys. Rev. A **38**, 4481, Nov. 1, 1988. "Relaxation of Gaseous Spin-Polarized ^{3}He Targets Due to Creation of $^3He^+$".

2. K.D. Bonin and M. A. Kadar-Kallen, Opt. News **14**, 41 (Dec. 1988). "Focusing Neutral Atoms".

3. K. D. Bonin, M. Gatzke, C. Collins, M. A. Kadar-Kallen, Phys. Rev. A **39**, 5624, June 1, 1989. "Absolute Photoionization Cross Sections of the Cs $7D_{3/2}$ Level Measured by Use of Fluorescence Reduction".

4. M. A. Kadar-Kallen and K. D. Bonin, Appl. Phys. Lett. **54**, 2296, June 5, 1989. "Focusing of Particle Beams Using Two-Stage Laser Ablation".

5. K. D. Bonin, M. Gatzke, C. L. Collins, and M. A. Kadar-Kallen, Sixteenth International Conference on the Physics of Electron and Atomic Collisions - Abstracts of Contributed Papers, July 26-August 1, 1989, A. Dalgarno, et al (ed.), p 12. "A Technique for Measuring Absolute Photoionization Cross Sections of Excited Atoms Using Fluorescence Reduction"

6. M. A. Kadar-Kallen and K. D. Bonin, Sixteenth International Conference on the Physics of Electron and Atomic Collisions - Abstracts of Contributed Papers, July 26-August 1, 1989, A. Dalgarno, et al (ed.), p 815. "Focused Particle Beams Produced by Two-Stage Laser Ablation" .

7. K. D. Bonin and M. Kadar-Kallen, Appl. Opt. **28**, 5293, December 15, 1989. "A Simple Diffuser for Production of Laser Speckle".

8. K. D. Bonin and W. Happer in *Encyclopedia of Applied Physics*, ed. George L. Trigg and Eduardo S. Vera (AIP, New York, 1991), approx. 30 pages (accepted Oct. 1990). "Atomic Spectroscopy".

9. K.D. Bonin and T.G. Mason, Phys. Rev. A15 **43**, to appear in March 15, 1991 issue. "Changing Fluorescence in a Streaming Barium Plasma Due to an Axial Magnetic Field". "A Narrowband, Tunable Pulsed Diode Laser near 900 nm".

10. K. D. Bonin and T. G. Mason, submitted to Seventeenth International Conference on the Physics of Electron and Atomic Collisions - Abstracts of Contributed Papers, July 10-15, 1991. "Changing Fluorescence in a Laser-produced Barium Beam Due to an Axial Magnetic Field".

11. K.D. Bonin, C.L.A. Collins, and M. Kadar-Kallen, and S.L. Keller, to be submitted to App. Opt., February, 1991. "A Narrowband, Tunable Pulsed Diode Laser near 900 nm".

2.6. List of Participating Scientific Personnel

1. Will Happer - Professor.

2. Keith Bonin - Assistant Professor.

3. Thad Walker - Postdoctoral Research Associate and Graduate Student - Received Ph.D. in Physics, January, 1988.

4. Michael Kadar-Kallen - Graduate Student.

5. Michael Gatzke - Graduate Student - Received Masters in Physics, May, 1989.

6. Carl Collins - Graduate Student - Received Masters in Physics, May, 1990.

7. Thomas Mason - Graduate Student.

8. Sarah Keller - Graduate Student.

9. Michael Fitch - Undergraduate Student.

10. David P. Saltzberg - Undergraduate Student.

11. John S. Allen - Undergraduate Student.

3. Report of Inventions

None.

4. Endnotes and Bibliography

[1]K. D. Bonin, M. Gatzke, C.L. Collins, and M.A. Kadar-Kallen, Phys. Rev. A. **39**, 5624(1989).

[2]A.Burgess and M.Seaton, Mon.Not.Roy.Astr.Soc.**120**, 121(1960).

[3]M.A.Kadar-Kallen and K.D.Bonin, Appl.Phys.Lett. **54**, 2296(1989).

[4]J. Maya and R. Lagushenko, in *Advances in Atomic, Molecular, and Optical Physics*, edited by B. Bederson and A. Dalgarno, (Academic Press, Orlando, 1990), pp.346-349.

[5]K.D. Bonin and T.G. Mason, Phys. Rev. A15, **43** ,1991.

Submitted February 11, 1991.